CrossMark

ORIGINAL ARTICLE

On the origin of the slow M–T chlorophyll *a* fluorescence decline in cyanobacteria: interplay of short-term light-responses

Gábor Bernát[1] · Gábor Steinbach[1,2] · Radek Kaňa[1] · Govindjee[3] ·
Amarendra N. Misra[4,5] · Ondřej Prašil[1,6]

Abstract The slow kinetic phases of the chlorophyll *a* fluorescence transient (induction) are valuable tools in studying dynamic regulation of light harvesting, light energy distribution between photosystems, and heat dissipation in photosynthetic organisms. However, the origin of these phases are not yet fully understood. This is especially true in the case of prokaryotic oxygenic photoautotrophs, the cyanobacteria. To understand the origin of the slowest (tens of minutes) kinetic phase, the M–T fluorescence decline, in the context of light acclimation of these globally important microorganisms, we have compared spectrally resolved fluorescence induction data from the wild type *Synechocystis* sp. PCC 6803 cells, using orange ($\lambda = 593$ nm) actinic light, with those of mutants, $\Delta apcD$ and ΔOCP, that are unable to perform either state transition or fluorescence quenching by orange carotenoid protein (OCP), respectively. Our results suggest a multiple origin of the M–T decline and reveal a complex interplay of various known regulatory processes in maintaining the redox homeostasis of a cyanobacterial cell. In addition, they lead us to suggest that a new type of regulatory process, operating on the timescale of minutes to hours, is involved in dissipating excess light energy in cyanobacteria.

Keywords *Synechocystis* · Fluorescence quenching · Kautsky effect · The M–T phase · Photoprotection · Interplay of regulatory processes

This paper is dedicated to the memory of our dear friend and colleague Fabrice Rappaport, who passed away on January 12, 2016.

✉ Gábor Bernát
bernat@alga.cz

[1] Laboratory of Photosynthesis, Institute of Microbiology, Academy of Sciences, Opatovicky mlyn, 379 81 Třeboň, Czech Republic

[2] Institute of Biophysics, Biological Research Centre, Hungarian Academy of Sciences, Temesvári krt. 62, Szeged 6726, Hungary

[3] Department of Biochemistry and Department of Plant Biology, University of Illinois at Urbana-Champaign, Urbana, IL 61801-3707, USA

[4] Centre for Life Sciences, Central University of Jharkand, Ranchi 835205, Jharkand, India

[5] Khallikote Cluster University, Berhampur 76001, Odisha, India

[6] Faculty of Sciences, University of South Bohemia in České Budějovice, 37005 Ceske Budejovice, Czech Republic

Abbreviations

Chl	Chlorophyll
Chl F	Chl *a* fluorescence
DCMU	3-(3′,4′-Dichlorophenyl)-1,1-dimethylurea
Flv	Flavodiiron (protein)
NPQ	Non-photochemical quenching of Chl F
OCP	Orange carotenoid protein
PBS	Phycobilisome
PQ/PQH$_2$	Plastoquinone/plastoquinol
PS	Photosystem
Q$_A$ and Q$_B$	The primary and secondary quinone electron acceptors of PS II
qE	Energy dependent quenching of Chl F
qI	Quenching of Chl F due to photoinhibition
qT	Quenching of Chl F due to state 1 to state 2 transition
SRFI	Spectrally resolved fluorescence induction
TL	Thermoluminescence

Springer

Introduction

Upon illumination of dark-adapted plant leaves, algae, and cyanobacteria, chlorophyll *a* fluorescence (Chl F) changes, in a characteristic manner, with time (the so-called Kautsky transient, known after Hans Kautsky) with several kinetic phases, which provide valuable information on photosynthesis and related processes including photo-adaptation and stress responses (for reviews, see e.g., Govindjee et al. 1986; Strasser et al. 2004; Papageorgiou et al. 2007; Papageorgiou and Govindjee 2011). Chl F measurement has been used as a highly sensitive, and a non-invasive tool in photosynthesis research for more than 60 years. In spite of this, there are still many open questions. Not only the origin of the slow (min) fluorescence transients (this paper), but even the most characterized fast (ms–s) transients are not yet fully understood (see below).

Usually six kinetic phases of the variable Chl F transient, labeled as O–J–I–P–S–M–T, are distinguished, which follow stepwise changes from the fast O–J rise (~ 1 ms) to the final very slow M–T decay (tens of minutes; for an example, see Fig. 1). During the first three steps (the so-called O–J–I–P rise) Chl F increases from the initial (minimal) O level through two inflection points (i.e. intermediate states) to a peak (P) level (see Fig. 1), where, the O–J step (the so-called *photochemical phase*) related to the reduction of Q_A, the primary quinone electron acceptor of photosystem II (PS II). The origin of the subsequent J–I–P rise (the so-called *thermal phase*) is still controversial, although it includes the reduction of the plastoquinone (PQ) pool, the effects of the formation of a membrane potential ($\Delta\Psi$) and/ or an undefined conformational change within PS II, as well as reactions leading to the filling-up of the electron acceptor side of PS I (see Samson et al. 1999; Schreiber 2002; Stirbet and Govindjee 2011, 2012; Vredenberg and Prašil 2013; Schansker et al. 2014; Hamdani et al. 2015; Kaňa and Govindjee 2016, and references therein; also see Laisk and Oja 2017). This rise is usually followed by the P–S phase, with S being a "local" minimum or a shoulder, also referred to as a "semi-steady" state (Fig. 1). This phase has a complex origin in which the formation of a trans-thylakoid pH gradient and reoxidation of Q_A^- (via PS I) are thought to play a major role (Briantais et al. 1986; Papageorgiou et al. 2007; Stamatakis and Papageorgiou 2014; for subphases between P and S, see Fratamico et al. 2016). The shape of the subsequent slow (S–M–T) phase is highly variable, depending on the organism and the light intensity used. While in higher plants, green algae and phycobilisome (PBS)-less cyanobacteria, such as *Prochlorococcus* sp., P is the major peak in the fluorescence transient and is often followed by a monotonous decrease of the signal to the T level; in cyanobacteria containing PBS antenna, P is only a "local" maximum followed (after the P–S phase) by a subsequent slow
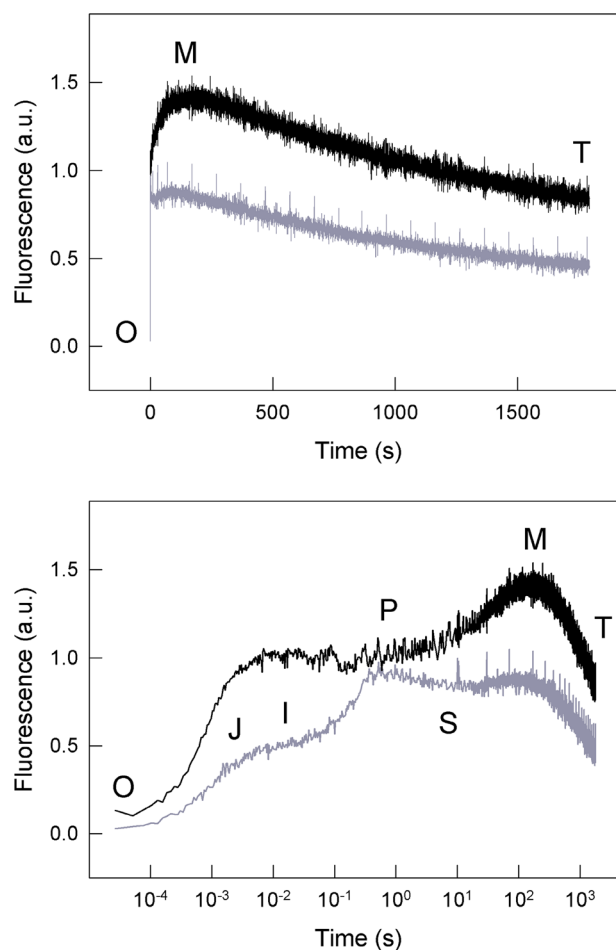

Fig. 1 Chl F transients in wild type *Synechocystis* cells in the absence (grey) and in the presence (black) of 10 µM DCMU and 1 mM KCN. Chl F was recorded after 10 min dark adaptation and plotted on a linear (top) and a logarithmic (bottom) time scale. Samples were excited by orange actinic light ($\lambda = 593$ nm; 750 µmol photons m^{-2} s^{-1}). Traces are normalized to the maximal fluorescence obtained upon a saturating pulse in darkness given 5 s before the fluorescence transients were recorded

(tens of seconds) S–M rise to a much higher maximum, the M level (Papageorgiou and Govindjee 1968; Papageorgiou et al. 2007; Stamatakis et al. 2007; Kaňa et al. 2009, 2012; Fig. 1). This rise was shown to reflect state 2 to state 1 transition in several photosynthetic organisms (Papageorgiou et al. 2007); this interpretation has been conclusively confirmed in the cyanobacterium *Synechocystis* sp. PCC 6803 (Kaňa et al. 2012), in several red algae including *Porphyridium cruentum* (Kaňa et al. 2014) as well as in the green alga *Chlamydomonas reinhardtii* (Kodru et al. 2015).

In higher plants, the slowest M–T (or P–T) kinetic phase, referred to, in the literature, as "decay", "decrease", or "decline", has several overlapping components whose relative contributions depend on light intensity, the organism used, history, and physiological/stress conditions. In this

paper, we have chosen to use, for the M-T phase, mostly M-T decline. At both low and high light intensities, non-photochemical quenching (NPQ) of the excited state of Chl *a* is the dominant contributor to the P–T decline, though at low light intensities, photochemical quenching (qP) also plays a significant role (Bradbury and Baker 1984). Phenomenologically, the NPQ itself consists of three major components: (1) energy-dependent quenching (qE), (2) state 1 to state 2 transition (qT), and (3) photoinhibition (qI) (Horton and Hague 1988; for reviews, see Horton 2014; Murchie and Harbinson 2014). These components are listed in the order of their relaxation kinetics (see Müller et al. 2001), where qE and qT have a fast and an intermediate relaxation kinetics, respectively, with approximate half-times of 0.5–2 min and 5–10 min, while the relaxation of qI takes hours. Although at certain light intensity, one or the other process predominates (qT at very low, and qI at high irradiance) qE develops and increases above a certain light level (Murchie and Harbinson 2014). In general, qT and qE are considered as manifestations of two distinct photoprotective/regulatory processes, while qI reflects the damage of PS II under strong light. We note that different from qE, qT may reflect changes mainly in Chl concentration, not in fluorescence lifetime (see e.g., Holub et al. 2007). In-depth investigations of these phenomena have indeed provided information on the molecular basis of quenching processes in higher plants (for reviews, see e.g. Lemeille and Rochaix 2010; Minagawa 2011; Brooks et al. 2014; Tyystjärvi 2013). Both photoprotective and regulatory quenching processes (i.e. qT and qE) have well-defined signal transduction pathways induced by plastoquinol (PQH_2) binding to the cytochrome b_6f complex, and the formation of a pH-gradient leading to a partial antenna relocation from PS II to PS I and an enhanced heat dissipation of the absorbed light via the major light harvesting protein complex of PS II (LHCII) (Lemeille and Rochaix 2010; Minagawa 2011; Brooks et al. 2014; Horton 2014; Holzwarth and Jahns 2014). Crucial components of these processes include Stt7/STN7 kinase (in the case of state transitions), the PsbS subunit of PS II, and the violaxanthin–antheraxanthin–zeaxanthin (VAZ) cycle (for energy-dependent quenching). Two other slowly relaxing components, qM and qZ, have also been observed. While qM was described as a consequence of chloroplast relocation inside plant cells upon irradiation (Dall'Osto et al. 2014), qZ was considered to be a zeaxanthin-dependent (but PsbS-independent) part of qE (Dall'Osto et al. 2005; Nilkens et al. 2010; Garcia-Mendoza et al. 2011; also see Puthiyaveetil et al. 2012, and Holzwarth and Jahns 2014 for further discussion).

The etiology of the M–T decay in cyanobacteria is not yet fully understood. First, all but one (i.e. state transition) of the above mentioned photoprotective and regulatory processes are associated with inherent features of green algae and higher plants, i.e., phosphorylation of LHCII, the major

light harvesting antenna, and retention of a specific organelle (i.e. chloroplast). Second, different from higher plants and green algae that are usually in state 1 in darkness and are shifted to state 2 upon illumination, dark-adapted cyanobacteria are usually in state 2 due to high rate of electron flow from metabolic pathways to the PQ-pool and they go to state 1 upon illumination due to their high PS I to PS II ratio and, in response to, strong oxidation potential of PS I (Mullineaux and Allen 1986; Mao et al. 2002). Thus, we suggest that although phenomenologically all oxygenic photosynthetic systems are quite similar, the origin of the M–T phase in cyanobacteria may be different, i.e., different components may predominate here than in higher plants (see above). Nevertheless, by analogy, one can expect that this M to T phase might also be related to short (or intermediate)-term light responses and/or photoinhibition.

In several cyanobacteria, orange carotenoid protein (OCP) is a key player in short-term light responses; in-depth investigation has revealed molecular details of this quenching process (Wilson et al. 2006; for a review see Kirilovsky et al. 2014). This type of quenching can exclusively be triggered by blue or blue–green light absorbed by the carotenoid in OCP, which converts it from an inactive orange form (OCP[o]) to an active red form (OCP[r]) (Wilson et al. 2008). Evidently, OCP quenching can account for a dominant fraction of NPQ (and, thus, it could possibly be involved in the M–T fluorescence phase) in cyanobacteria upon illumination with blue/blue–green light (El Bissati et al. 2000). However, the M–T decline may also be induced by strong orange light (*this work*), which suggests a substantial contribution of an OCP-independent process to be responsible for the M–T phase in cyanobacteria. A new type of cyanobacterial short-term regulatory processes has now been found in which the reaction centers are protected against excess light by energetic decoupling and subsequent detachment of PBSs from the thylakoid membranes, induced by local heat transients within the antenna (Stoitchkova et al. 2007; Kaňa et al. 2009, 2012; Tamary et al. 2012; Steinbach and Kaňa 2016; for a review, see Kirilovsky et al. 2014). Also, photoprotective reaction center type quenching has been established in an extremophile cyanobacterium (Ohad et al. 2010) and in a red alga (Krupnik et al. 2013). Our data suggest that besides photoinhibition and OCP quenching, other regulatory short-term processes must also be considered to fully explain the M–T phase in *Synechocystis* sp. PCC 6803.

Materials and methods

Cyanobacteria and their culture conditions

Wild type and mutant cells of *Synechocystis* sp. PCC 6803 (referred simply as *Synechocystis* hereafter) were grown

at 28 °C in standard BG11 medium (Stanier et al. 1971; cf. http://www-cyanosite.bio.purdue.edu/media/table/BG11.html) in Erlenmeyer flasks under continuous illumination (40 µmol photons m^{-2} s^{-1}) of white fluorescence light. Mutants, unable to perform either state transitions ($\Delta apcD$) or OCP quenching (ΔOCP), used in this study, were gifts of Diana Kirilovsky (Centre Energie Atomique (CEA), Saclay, Gif sur Yvette, France); for details of these mutants, see Jallet et al. (2012) and Wilson et al. (2006). In addition to the above-mentioned mutants, we have also used a PBS-less PAL mutant, which was originally obtained by Ajlani and Vernotte (1998) by deletion of the *apcAB* operon. Solid stock cultures were kept on agar plates. Except for the experiments with the slowly growing PAL strain, where we used 8–10 day old cultures, 4–5 day old cultures were used in all other experiments described in this paper.

Recording of conventional and spectrally resolved fluorescence induction curves

Chl F induction curves were recorded using a FL-100 Fluorometer [Photon Systems Instruments (PSI), Brno, Czech Republic]. Simultaneously, spectrally resolved fluorescence induction (SRFI) curves were measured using a SM-9000 spectrophotometer (PSI; 5 Hz, 100 ms integration periods, followed by a 100 ms pause) triggered by FL-100. Kaňa et al. (2012) have described both the experimental protocol and the instrumentation, used here. Samples were kept in darkness for 10 min, and then fluorescence induction curves were recorded up to 30 min. The chosen duration was used as a compromise between the capability of our experimental setup and the kinetics of the explored phenomenon. Excitation of the sample was by orange ($\lambda = 593$ nm) measuring light (< 0.5 µmol photons m^{-2} s^{-1}) as well as actinic light (750 µmol photons m^{-2} s^{-1}); further, saturating pulses ($\lambda = 593$ nm; $I = 1250$ µmol photons m^{-2} s^{-1}; $\Delta t = 600$ ms) were given on top of the actinic light. In order to avoid sedimentation of cells, a magnetic bar was used to stir the samples during data acquisition. The two perpendicular cross sections of the SRFI datasets, i.e., room temperature fluorescence emission spectra and induction curves, were evaluated using a custom-written software. Since FL-100 detects modulated fluorescence emission between 700 and 750 nm (Nedbal and Trtílek 1995), it measures Chl F, whereas, SRFI dataset covers a much broader spectral range (see "Results").

Samples for measuring low temperature (77 K) fluorescence emission spectra, thermoluminescence (TL), and oxygen yields were used after 10 min of dark incubation, as well as after 100 and 1800 s of the onset of the actinic light, representing the O, M and T phases, respectively, of fluorescence induction (transient).

Low temperature fluorescence emission spectroscopy

150 µL of cell suspension was collected at three defined time points before and during the accumulation of SRFI datasets (see above) and loaded into the cavity of a copper finger of home-made apparatus, described by Prášil et al. (2009). Trapping of the samples, at O, M and T steps of fluorescence induction, was achieved by rapid freezing in a transparent Dewar flask filled with liquid nitrogen. 77 K fluorescence emission spectra were recorded using an SM-9000 spectrophotometer (Prášil et al. 2009) upon excitation with 588 nm light (bandwidth = 20 nm). Three individual spectra of each sample were recorded and averaged.

Thermoluminescence (TL)

TL glow curves were recorded using a Thermoluminescence System TL 200/PMT (PSI), as described by Belgio et al. (2017). Immediately after sample collection (see "Recording of conventional and spectrally resolved fluorescence induction curves" section), 1 mL of cell suspension was filtered through a #5 nitrocellulose membrane filter (pore size: 0.6 ± 0.1 µm; Pragopor, Czech Republic) and placed onto the sample holder. Samples were cooled down to 3 °C, where two subsequent saturating single turnover flashes (50 µs, 200 ms apart) were given 1 s prior to the start of the heating and recording phase. TL curves were recorded from 3 to 65 °C with a heating rate of 0.5 °C s^{-1}.

Oxygen yield measurements

Rates of oxygen evolution and consumption were measured in 1 mL cell suspensions of *Synechocystis*, using a Clark-type oxygen microelectrode (MI-730 Dip-type O_2 Microelectrode, Microelectrodes, Inc., USA). The signal was amplified and digitized using the Oxycorder 301 (PSI, Czech Republic). Activities of the whole linear electron transport chain from water to CO_2 were measured in the presence of 10 mM $NaHCO_3$. Rates of photosynthesis were obtained from the difference of the net oxygen evolution in light and the oxygen consumption in the dark. A KL 1500 LCD fiber optic halogen lamp (Schott, Mainz, Germany) was used to provide saturating white light (500 µmol photons m^{-2} s^{-1}) in these experiments.

Results

Chl F transient in *Synechocystis* with and without DCMU and KCN

Typical Chl F induction curves of untreated *Synechocystis* cells after exposure to 750 µmol photons m^{-2} s^{-1} orange

(593 nm) actinic light, for 30 min, are shown in Fig. 1 (grey curves); see "Introduction". When fluorescence is plotted on a linear time scale (top panel), an unresolved rise to a maximum M (at around 80–100 s) is observed which is followed by a slower monotonous decrease towards a terminal steady state level T. Note that reaching a steady state T level would need a very long time (hours); however, due to the quasi-exponential character of this terminal phase, we compromised the time of recording to ~ 1800 s (~ 30 min), which still provided sufficient information on the M–T phase (see below). Hence, the symbol "T" here and thereafter should be interpreted as "towards T". The relaxation time of the M–T phase is long (>> 30 min) and requires light (data not shown). The fast components of the fluorescence transients are clearly observed by plotting the same data on a logarithmic time scale (Fig. 1, bottom panel; see "Introduction"). Besides the O (also referred to as F_O), the M, and T levels, we clearly observe the fast O–J–I–P–S fluorescence transient (for the origin and nomenclature of the individual steps, see "Introduction"). Although the shape of this induction curve is characteristic and quite similar to those previously published (see e.g. Kaňa et al. 2012), yet we observed some variations in the intensity at the M level (data not shown). We speculate that these variations may have been due to possible variations in the PQ/PQH_2 redox levels in the different samples. In order to decrease this variability and to maximize the S–M rise, both KCN and 3-(3,4-dichlorophenyl)-1,1-dimethylurea (DCMU) were added, the former blocking respiration, and preventing PQH_2 re-oxidation by terminal oxidases in darkness, while the latter blocking electron flow beyond Q_A because of its binding to the Q_B site, and, thus, preventing the reduction of the PQ pool by PS II upon illumination (see Bernát et al. 2009, 2011, and the literature cited). Hence, in the presence of KCN and DCMU, the reduced PQ-pool in darkness is effectively re-oxidized, via PSI, upon illumination. While this treatment (see black curves) leads to a fast, single-step O–P rise without the obvious J and I steps (Fig. 1, bottom), it also generates a large S–M rise (Kaňa et al. 2012) and a subsequent reversible[1] M–T decline (Fig. 1, bottom). At the intensity used in our experiment, about $38 \pm 4\%$ of the variable Chl F is decreased over the 30 min illumination period (Fig. 1).

---

[1] We checked the reversibility of the phenomenon by keeping the cells for 2 h in low light, and then measuring the fluorescence transient. We found that it was completely restored; further, the M–T phase could be induced again even in the presence of DCMU and KCN.
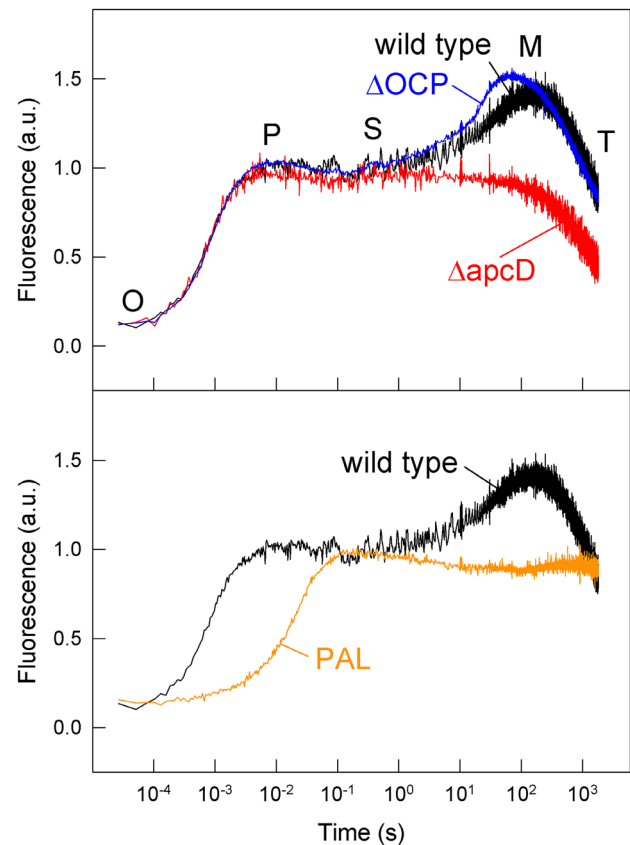

Fig. 2 Chl F transients in the wild type (black) and three different mutants of *Synechocystis*: ΔOCP (incapable of quenching of fluorescence by OCP; blue), Δ*apcD* (incapable of state transitions; red), and PAL (PBS-less; orange), in the presence of 10 µM DCMU and 1 mM KCN. The curve for ΔOCP was smoothened for clarity. For further details see the legend of Fig. 1

Chl F transients of three *Synechocystis* mutants: ΔOCP, Δ*apcD*, and PAL

In order to obtain an understanding of the potential contribution of several possible processes (e.g., qT, qI, OCP quenching, increased electron flow, and CO_2 assimilation, among others) to the M–T fluorescence phase, we measured the complete fluorescence transients of selected *Synechocystis* mutants: (1) Δ*apcD*, which is incapable of state transitions (Jallet et al. 2012); (2) ΔOCP, which is incapable of quenching of fluorescence by OCP (Wilson et al. 2006); and (3) PAL, which is a PBS-less mutant (Ajlani and Vernotte 1998). As shown already in Fig. 1, we recorded these curves in the presence of DCMU and KCN. The pattern of the fluorescence induction curve of ΔOCP cells (Fig. 2, top panel, blue line) is very similar to that of the wild type (black), which shows that ΔOCP cells are able to perform state transitions on the one hand, and, on the other hand, it suggests that the M–T phase is not due to quenching of fluorescence by OCP when orange actinic light is used, which

does not trigger OCP activation. Interestingly, both the S–M rise and the M–T decline are more pronounced in the ΔOCP mutant than in the wild type (for M–T decay: 45 ± 4 vs. $38 \pm 4\%$ decrease of Chl F). On the contrary, Δ*apcD* shows a monotonous decrease towards the T level after the S level had been reached (red); this is in good agreement with the current view that the S–M rise is due to state 2 to state 1 transition (Papageorgiou et al. 2007; Kaňa et al. 2012; Kodru et al. 2015; Stirbet and Govindjee 2016). Here again, the quenching of Chl F is much higher ($50 \pm 3\%$) than in the wild type. Nevertheless, the occurrence of the M–T fluorescence decay in these strains clearly suggests that although both state 1 to state 2 transition and OCP quenching might contribute to the M–T decline in the wild type *Synechocystis* under certain circumstances, at least one additional process must also be involved in the underlying mechanism. Different from these strains, the fluorescence transient of the PBS-less PAL mutant shows no significant change in the fluorescence yield after reaching the P level (Fig. 2, bottom panel, orange curve). Since the PAL mutant has rather low light absorption at 593 nm (Bernát et al. 2009), the P level is delayed here, appearing at 170 ms instead of 10 ms, as in other strains. Thus, we asked if the lack of the M level in the PAL strain might be a consequence of low antenna cross section and/or an insufficiently short recording time. However, since no fluorescence decrease in this strain has been observed even with intense (1700 μmol photons m^{-2} s^{-1}) blue–green light (Wilson et al. 2006), we conclude that the PAL mutant is indeed unable to show the S–(M)–T phase. This suggests that PBS antenna must be involved in the underlying molecular processes that control fluorescence transient in cyanobacteria.

Spectrally resolved fluorescence induction (SRFI)

As already mentioned in "Recording of conventional and spectrally resolved fluorescence induction curves" section, fluorescence transients, shown in Figs. 1 and 2, correspond to integrated fluorescence emission over the spectral region from 700 to 750 nm (Nedbal and Trtílek 1995). For further insight into processes behind the phenomenon, 3D (time vs. wavelength vs. intensity) SRFI datasets were constructed by repeated recording of about 9000 consecutive room temperature fluorescence emission spectra during the fluorescence transient, as obtained by illuminating the samples with orange actinic light. The perpendicular cross section of these datasets "visualizes" fluorescence induction curves at particular wavelengths (for a detailed description of the method, see Kaňa et al. 2009, 2012). Figure 3 shows fluorescence transients of wild type, ΔOCP, and Δ*apcD* cells obtained by this method at three selected wavelengths: 658 nm (for phycobilin fluorescence), 682 nm (for Chl F, mainly from PS II) and 745 nm (mainly the vibrational satellite band

of Chl F from both PS II and PS I) (see e.g., chapters in Govindjee et al. 1986; and Papageorgiou and Govindjee 2004; also see Fig. 4). Importantly, these measurements were performed with non-modulated fluorescence detection (i.e. without any measuring light), where fluorescence emission was directly generated by excitation with actinic light (750 μmol photons m^{-2} s^{-1}) and saturating light pulses (1250 μmol photons m^{-2} s^{-1}). Therefore, F_O (O), F_T and F'_M levels, obtained by this method, are not comparable without correction (with other data), as, besides inherent changes in fluorescence emission, they also reflect differences in intensities of fluorescence excitation. However, as shown in Figs. 1 and 2, applying saturation flashes in the presence of DCMU and KCN does not induce any real increase in the fluorescence yield, and the shapes of the S–(M)–T fluorescence curves are quite similar, irrespective of whether the cells are excited with 750 μmol photons m^{-2} s^{-1} or on-top with 1250 μmol photons m^{-2} s^{-1} light pulses.

In wild type *Synechocystis* cells, both the S–M rise and the subsequent M–T decrease are observed at all the three wavelengths used here (Fig. 3, left column); the relative S–M increase and the M–T decrease of the fluorescence intensity are much larger at 682 nm ($27 \pm 4\%$ increase and $25 \pm 4\%$ decrease), than at 745 nm ($22 \pm 2\%$ increase and $21 \pm 2\%$ decrease) and at 658 nm ($11 \pm 1\%$ increase and $12 \pm 1\%$ decrease). (Note that these numbers refer to changes in F'_M; therefore, they cannot be directly compared with the changes in fluorescence, shown in Figs. 1 and 2). A similar but much more pronounced effect was observed in ΔOCP cells: $35 \pm 5\%$ increase of the fluorescence yield during the S–M rise and $29 \pm 3\%$ decrease during the M–T phase at 682 nm; $26 \pm 3\%$ increase and $23 \pm 3\%$ decrease at 745 nm; and $13 \pm 1\%$ increase and $11 \pm 1\%$ decrease at 658 nm (Fig. 3, middle column). In contrast, the M peak is missing from the corresponding fluorescence induction curve of the Δ*apcD* strain (Fig. 3, right column). These findings are in agreement with those obtained from conventional measurements of fluorescence (Fig. 2, see also Kaňa et al. 2012). Nevertheless, the decreasing part of fluorescence transient in the Δ*apcD* strain is similar to those observed in other strains. Here, again, the relative decrease of the fluorescence intensity during the decay to the T level was much higher when measured at 682 nm ($32 \pm 3\%$), than at 745 nm ($25 \pm 3\%$) and 658 nm ($13 \pm 1\%$). These observations show that the fluorescence decrease to T level occurs in all the investigated strains and that it is highest around 682 nm, which originates from Chl *a* in PS II. Also, the effect is remarkably higher in the mutants unable to perform state transitions or OCP-dependent quenching (see below; "Analysis of non-photochemical quenching (NPQ) of Chl F" section), which suggests that these short-term processes have either a photoprotective role (e.g. if the decline to T
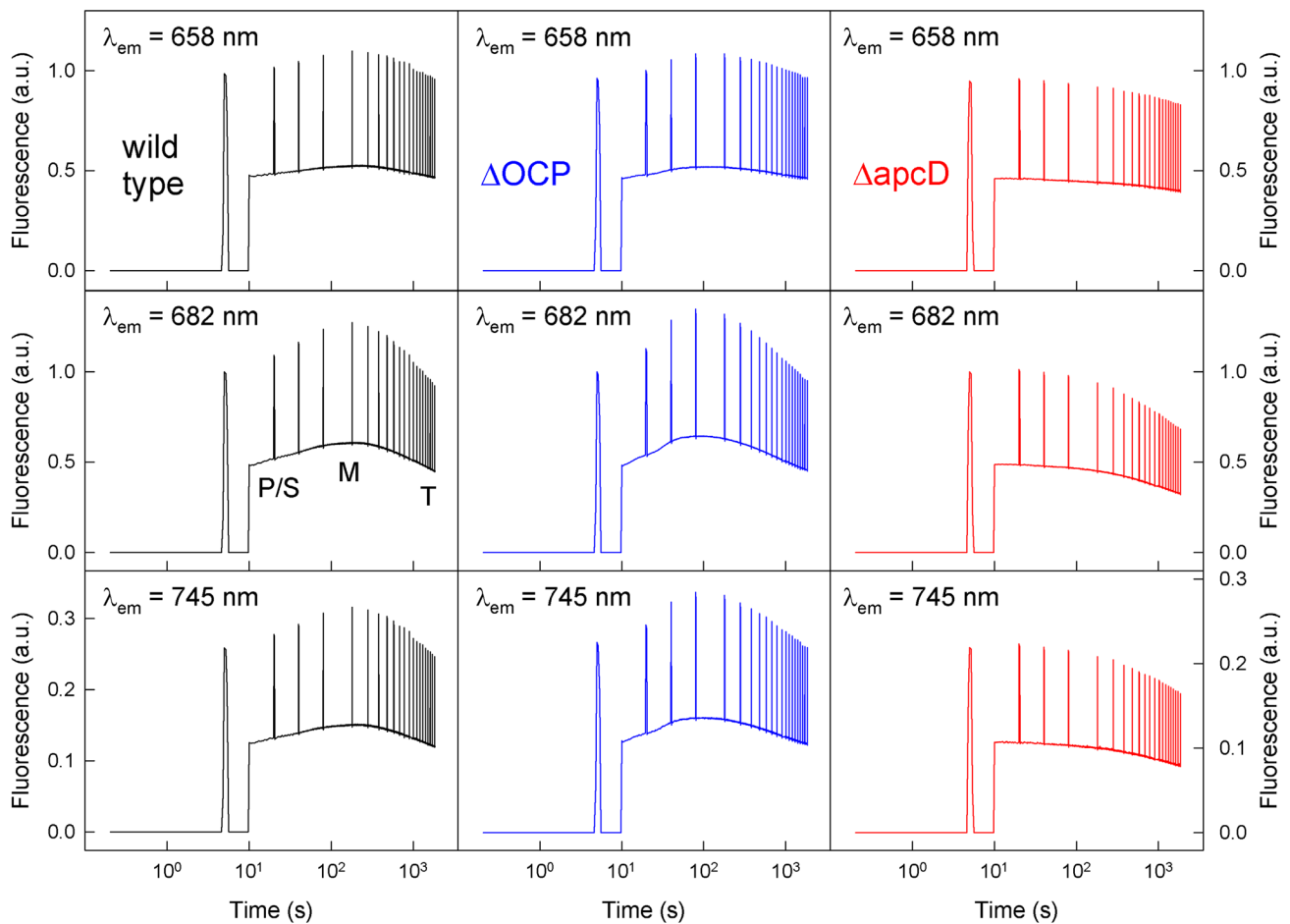
Fig. 3 Orange light induced fluorescence transients of wild type *Synechocystis* (left column), ΔOCP (middle column), and Δ*apcD* strain (right column) at three selected wavelengths (658 nm for phycobilin fluorescence; 682 nm for Chl F; and 745 nm for the vibrational satellite shoulder of Chl *a* band) in the presence of 10 μM DCMU (added to inhibit electron flow beyond Q$_A$) and 1 mM KCN (added to inhibit respiration). A series of 9000 consecutive room temperature fluorescence emission spectra (for examples, see Fig. 4.) were recorded in parallel with the fluorescence induction curves, shown in Figs. 1 and 2, at a frequency of 5 Hz. Fluorescence induction curves, at selected wavelengths, were constructed by 3D SRFI datasets. Note that apparent changes in fluorescence yields upon turning on the actinic light and at saturating pulses reflect mainly differences in the intensities of fluorescence excitation. For further details see text

reflects photodamage), or they are in a complex relationship with other protective responses (if the decrease to the T level reflects a protective mechanism). This assumed complex relationship is also supported by the more pronounced S–M rise of the ΔOCP strain (i.e. its inability for OCP-quenching, one major protective mechanism in *Synechocystis*, which seems to be compensated by a more prominent state 2 to state 1 transition), in agreement with data on cyanobacterial strains incapable of fluorescence quenching by OCP (Kaňa et al. 2012). As the M–T phase is completely missing in the PAL mutant (Fig. 2), we propose that this decrease in fluorescence might be connected with an OCP-independent PBS-related process.

SRFI: room temperature fluorescence emission spectra

Room temperature fluorescence emission spectra at selected time points of the same datasets, as discussed above, are shown in Fig. 4; these spectra were collected at 20, 80, and 1800 s after the start of the experiment, representing the S, M and T levels. The spectra (left columns) show emission peaks at 682 nm (from Chl *a* in PS II with a possible small contribution from the PBS terminal emitter), at 658 nm (from PBS), and a broad vibrational shoulder at 745 nm (mainly from Chl *a* in both PS II and PS I). In agreement with the data in Figs. 1, 2 and 3 (see above), the fluorescence yield of wild type cells (top left panel) increased
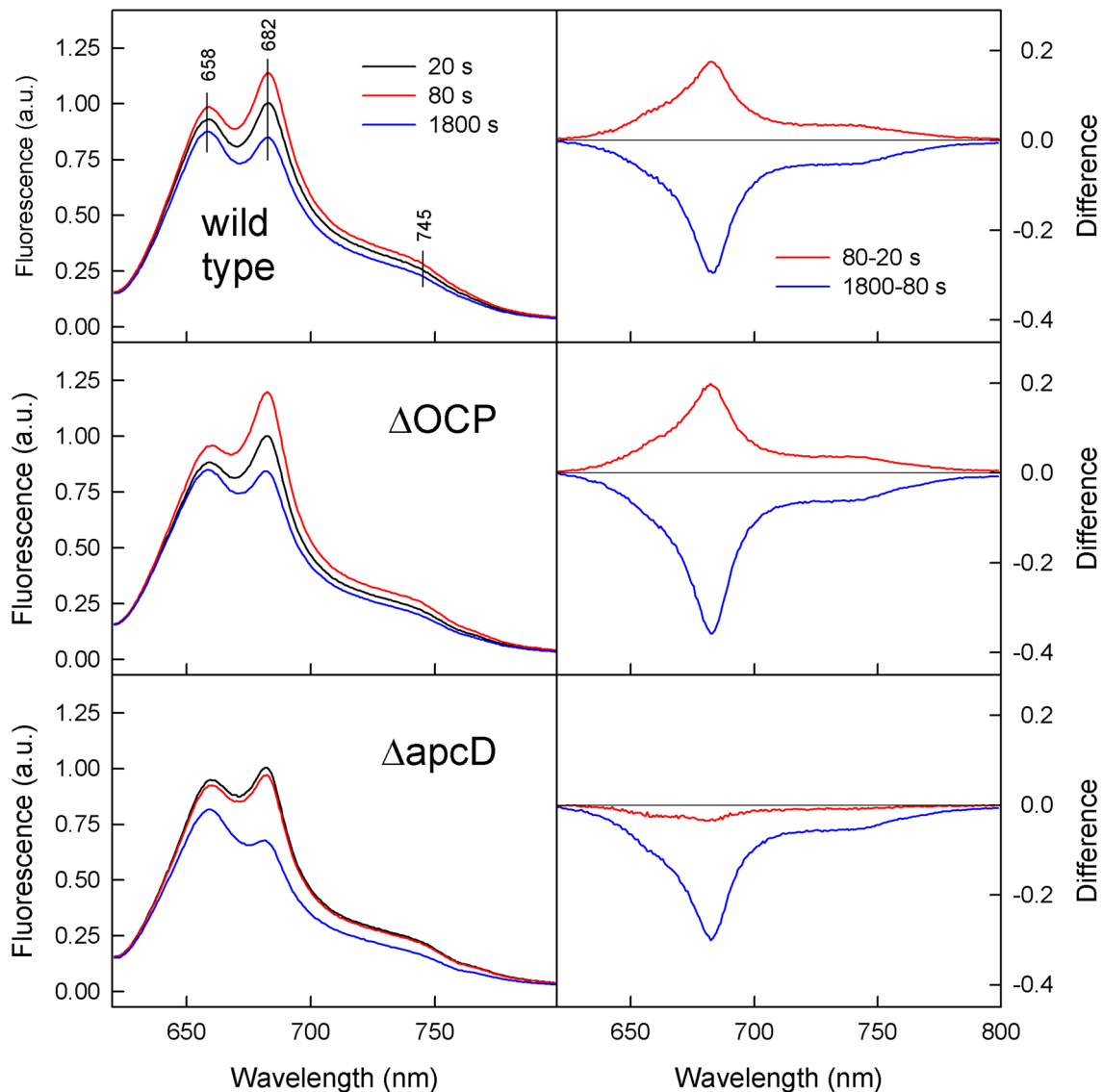
Fig. 4 Left panels: room temperature fluorescence emission spectra of the wild type and two mutants (ΔOCP and Δ*apcD*) of *Synechocystis* in the presence of 10 μM DCMU and 1 mM KCN, recorded at three selected time points, 20 s (for S; black), 80 s (for M; red), and 1800 s (for T; blue) after the orange actinic light was switched on (cf. Figs. 1 and 2). Right panels: difference emission spectra of those are shown in the left panels

considerably from the S level (black line) to the M level (red line), followed by a decrease to the T level (blue line). As already mentioned above, a more pronounced, but similar pattern was obtained in the ΔOCP strain with a maximal effect at 682 nm (middle left panel, cf. Fig. 2). On the contrary, and in agreement with data shown in Figs. 2 and 3, no fluorescence increase from 20 s (S level) to 80 s (M level) was observed in the Δ*apcD* cells (Fig. 4, bottom left panel) due to lack of state transitions (cf. Kaňa et al. 2012). However, the fluorescence decrease to the T level in this strain was similar to those obtained in the wild type and in ΔOCP strains (Fig. 4, left panels). The relative decrease of the fluorescence in the Δ*apcD* strain, again, is more

pronounced than that in the wild type cells, which suggests that state transition may have a photoprotective role (see "Discussion").

Differences of the fluorescence emission spectra, shown in the left panels of Fig. 4, are presented in the right panels of the same figure. These difference spectra show negligible changes at 658 nm (phycobilin fluorescence) both during the S–M rise (Fig. 4, right column, red lines) and the M–T decline (blue lines). However, changes in the fluorescence intensities at the 682 nm peak and the shoulder at 745 nm (Fig. 4, right column) are clearly high. Relative changes in fluorescence intensities are slightly higher at 682 nm than at 745 nm; this is in good agreement with the fact that the
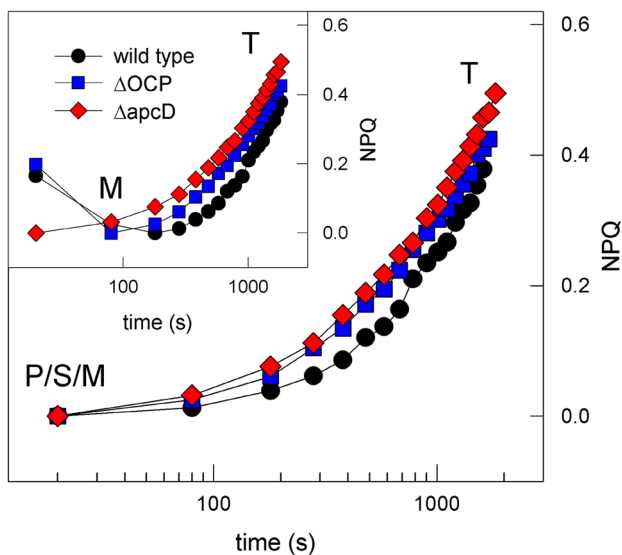
Fig. 5 NPQ in wild type *Synechocystis* (black dots) and in its mutant strains, ΔOCP (blue filled squares) and Δ*apcD* (red filled diamonds), as calculated from fluorescence induction curves, at 682 nm (shown in Figs. 3 and 4). The inset shows data on complete induction curves, whereas the main figure shows only the M–T or the S–T phase. See "Spectrally resolved fluorescence induction (SRFI)" and "Analysis of non-photochemical quenching (NPQ) of Chl F" section for further details

682 nm emission originates mostly from Chl *a* in PS II, whereas the vibrational satellite is due to Chl F from both PS II and PS I (see above). Hence, similar to the S–M rise, the M–T decline is also closely related to PS II. Again, the relative changes in fluorescence emission during both the S–M and the M–T phases in the ΔOCP strain and during the S–T phase in the Δ*apcD* strain was relatively higher than was observed in the wild type.

Non-photochemical quenching of Chl fluorescence

In order to quantify results presented in Figs. 3 and 4, we have calculated NPQ as:

$$NPQ = \left(F'_{M(max)} - F'_{M}\right)\Big/F'_{M}, \tag{1}$$

where $F'_{M\,(max)}$ is the maximum F'_{M} value during actinic illumination (Serôdio et al. 2006). (Usually, F_{M}, i.e., maximum fluorescence, after a dark period is used instead of $F'_{M\,(max)}$ (Demmig-Adams et al. 2014).) This approach is especially applicable for cyanobacteria, which, different from higher plants, have usually higher $F'_{M\,(max)}$ than F_{M} (Note, however, that due to the use of DCMU in our experiments, contribution of qP to the M–T phase is disregarded). The NPQ values deduced from fluorescence curves (see Fig. 3) are presented in the inset of Fig. 5. This reveals an increase in NPQ after it had reached a minimum value at the M level,

both in the wild type (black dots) and in ΔOCP mutant (blue filled squares). However, in the case of Δ*apcD*, there was a monotonous increase in NPQ during the S–T decline (red filled diamonds). Only the ascending parts of these curves are shown in the main panel of Fig. 5. Fitting these curves by exponential functions reveals higher rate constants of NPQ formation (and S/M–T decline) for the mutants than for the wild type: wild type, $2.85 \pm 0.46 \times 10^{-4}$ s^{-1}; ΔOCP, $3.44 \pm 0.39 \times 10^{-4}$ s^{-1}; Δ*apcD*, $3.86 \pm 0.36 \times 10^{-4}$ s^{-1}. Also, in agreement with the data shown in Figs. 3 and 4, both the inset and main panel show higher NPQ in the mutants that are unable to engage in OCP quenching or state transitions. This, again, clearly suggests the possible contribution of an unknown NPQ process and/or photoinhibition for the M–T phase when cells are exposed to orange actinic light. Even in the presence of DCMU, which prevents PQ reduction via PS II, state 1 to state 2 transition cannot be excluded, a priori, in the strains capable of state transitions since electron transport from metabolic reactions may reduce PQ. However, this possibility can be excluded as no state 1 to state 2 transition was observed through measurements of low temperature fluorescence emission spectra (see "Low temperature (77 K) fluorescence emission spectra" section).

Thermoluminescence (TL)

TL provides information on the back reactions of PS II components, especially between the S-states of the water oxidizing complex (WOC), and the reduced electron carriers Q_A and Q_B (see, e.g. DeVault and Govindjee 1990; Vass and Inoue 1992, and Vass and Govindjee 1996). While peak positions characterize the redox potential difference between the interacting components in the corresponding charge recombination, the peak intensities are affected by various processes; they provide information on PS II reactions, including radiative and non-radiative charge recombination steps, and even the antenna size. In order to obtain information on TL changes during the S–M rise and the M–T (or S–T) decrease, we used wild type and Δ*apcD* cells kept in darkness (representing the O level) as well as in light, representing the M (if any) and T levels. TL was then measured following flash illumination at 3 °C (Fig. 6). In all cases B-band(s) (B_1 and B_2), originating from $S_2Q_B^-/S_3Q_B^-$ charge recombination, were observed with a peak at about 20 °C. In agreement with a possible change due to state 2 to state 1 transition, the S–M transition led to a ~20% increase in the TL yield in the wild type, which was followed by ~30% decrease during the subsequent M–T phase (Fig. 6, top panel). The observed increase in the TL intensity is suggested to be due to an apparent increase in the antenna size of PS II (for a quantitative analysis of antenna cross section in state 2 and state 1, see Bernát et al. 2012). In agreement with this concept, we did not observe a similar
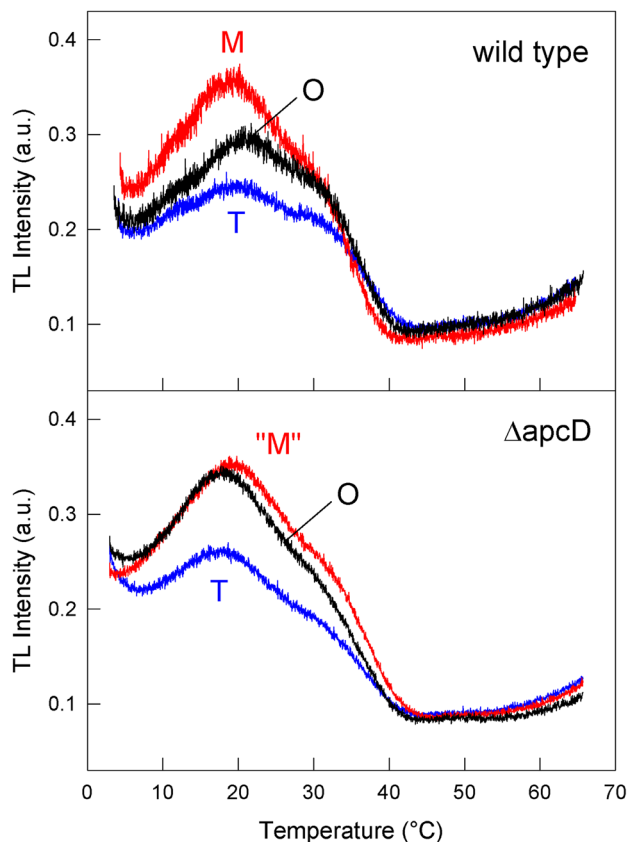
Fig. 6 TL curves of wild type (top) and Δ*apcD* (bottom) *Synechocystis* cells. Samples were collected after a 10 min dark period (for the O level; black), as well as after 100 s (for the M level, red) and 1800 s (for the T level; blue) of actinic light. The quotation marks on "M" inthe bottom panel was used to indicate that it could not be induced in the state transition mutant Δ*apcD*; however samples were taken when the M-peak appears in the wild type

increase in the TL-intensity in the Δ*apcD* mutant that lacked state transitions (Fig. 6, bottom panel). (For a theoretical discussion, see Rappaport and Lavergne 2009.) Further, the M–T (or S–T) decline may either reflect a decrease in the antenna cross-section or, less likely, a damage of the photosynthetic apparatus (see below). Alternatively, the observed decrease in TL intensity may represent the activation of a non-radiative pathway of charge recombination, which increases the phototolerance of cells under high light (Cser and Vass 2007).

Low temperature (77 K) fluorescence emission spectra

As mentioned above, one possible explanation for the formation of NPQ (Fig. 5) and accompanying decrease in TL-intensity during the M–T fluorescence decline (Fig. 6) is a quenching of the excited state of Chl *a*, the nature of which was investigated through 77 K spectra. Since we used orange ($\lambda = 593$ nm) actinic light, which is absorbed
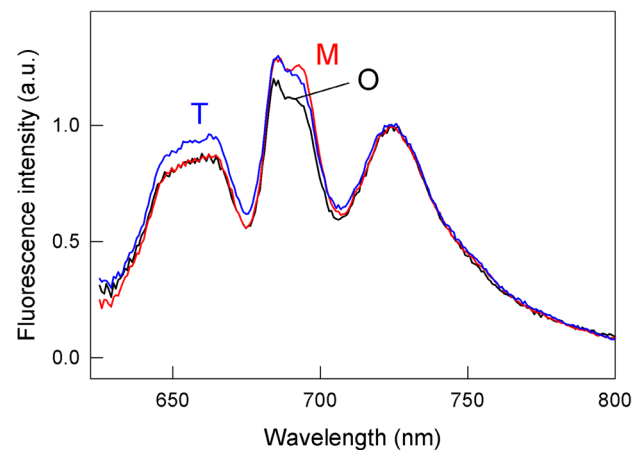

Fig. 7 Low temperature (77 K) fluorescence emission spectra of untreated wild type *Synechocystis* cells. Samples were collected after a 10 min dark period (for the O level; black), as well as after 100 s (for the M level; red) and 1800 s (for the T level; blue). Excitation light: 588 nm. Spectra were normalized at 725 nm

by phycobilins, the underlying quenching process is expected to be different from that when blue light, which is absorbed by OCP, is used. Stoitchkova et al. (2007), Küpper et al. (2009), Kaňa et al. (2009, 2012), Tamary et al. (2012) and Steinbach and Kaňa (2016) have suggested a regulated decoupling of PBS from the PS II reaction centers upon strong illumination. Potential decoupling of PBS during the M–T decline was examined by measuring 77 K fluorescence emission spectra at the O, M and T levels. After dark adaptation, emission spectrum (excitation wavelength: 588 nm) of the O level was obtained (Fig. 7, black line); it shows emission bands for phycocyanin (at 650 nm), for allophycocyanin (at 663 nm), for Chl *a* of PS II from 2 different components (685 and 693 nm) with a possible contribution from the PBS terminal emitter (at 685 nm), and from PSI (725 nm); Chl emission bands must arise by excitation energy transfer from phycobilins since excitation was at 588 nm. The emission spectra at the M level (Fig. 7, red line), as compared to that at the O level, show an increase in the Chl *a* emission from PS II, without any change in the phycocyanin and allophycocyanin fluorescence. The increase in the emission at 685 and 693 nm, as compared to that at 725 nm, is consistent with it being due to state 2 to state 1 transition (see, e.g. Bernát et al. 2009, 2012; Tsunoyama et al. 2009; Kaňa et al. 2012). Subsequent 30 min illumination with orange light did not cause any major change in the PBS to PS II excitation energy transfer (Fig. 7, blue line), indicating that the cells remained in state 1 even after prolonged illumination. However, substantial increase in fluorescence emission was observed in the PBS spectral region at 650–663 nm, suggesting a possible light induced partial decoupling of

PBS from the PS II reaction centers, similar to the findings of Stoitchkova et al. (2007). Correspondingly, the M–T transition was accompanied by an $8 \pm 1\%$ increase in the F685/F695 ratio. The observed change in the PBS versus Chl F is consistent with the room temperature fluorescence emission data (see Fig. 4 and "SRFI: Room temperature fluorescence emission spectra" section). However, the relatively small change (~ 10%) in PBS- as compared to Chl F suggests that this decoupling can account only for a minor fraction of the M–T phase under the (moderate) conditions used in this experiment.

Potential contribution of photoinhibition to the M–T phase

In order to explore the potential contribution of photoinhibition during the M–T phase, Chl F transients were recorded with and without a protein synthesis inhibitor, lincomycin (Fig. 8, top panel; the curve with lincomycin was arbitrarily shifted upwards for clarity). Lincomycin is known to prevent the PS II repair cycle, hence, enhancing photoinhibition (Allakhverdiev et al. 2002, 2005). As compared to control cells (black line), lincomycin had no effect on the fast fluorescence transient (green vs. black line). On the other hand, the M–T decline became steeper, as also observed in the curves calculated for NPQ (Fig. 8, middle panel). This remarkable increase in the M–T decay in the presence of lincomycin is also noticeable by comparing the corresponding difference fluorescence emission spectra recorded at room temperature (Fig. 8, bottom panel, 1800–80 s). Here again, in the presence of lincomycin, the decrease at the T level from that at the M level was the highest at 682 nm. This suggests that photoinhibition certainly contributes to the decrease from the M level to the T level, especially when the PS II turnover is prevented. In contrast to the differences in the M–T phase, the difference spectra over the O–(J–I–P–S)–M transition (80–20 s) were hardly different in the presence and the absence of lincomycin.

In order to examine the role of photoinhibition in the M–T phase in the absence of lincomycin, oxygen evolution of the cells was measured. As shown in Fig. 9, 30 min illumination of *Synechocystis* with strong orange light does not cause any change in the yield of oxygen evolution (striped vs. open white column), which is in good agreement with the data of e.g. Allakhverdiev et al. (2002). However, in the presence of lincomycin, illumination with intense orange light causes an about $15 \pm 4\%$ decrease of the oxygen yield (Fig. 9, striped green column). This indicates that contribution of photoinhibition to the M–T phase must be more pronounced under high light conditions, as expected.
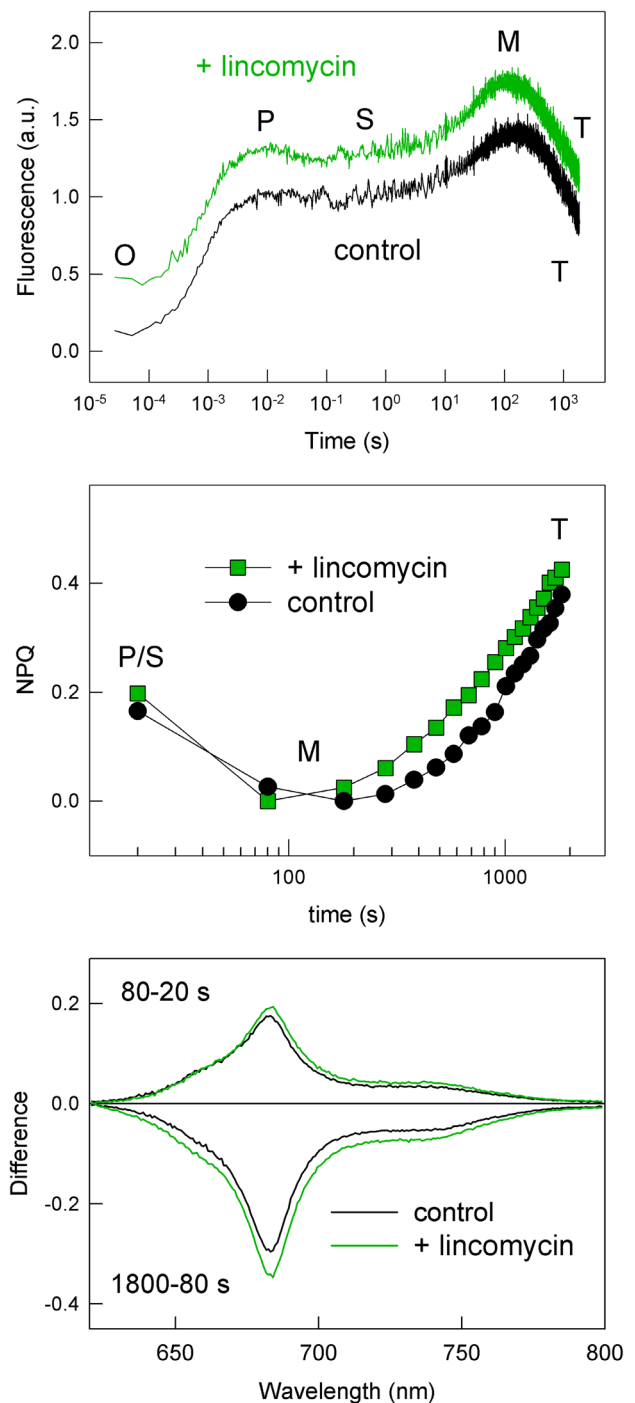

Fig. 8 Effect of 1.5 mM lincomycin on Chl F induction (top panel), on NPQ (middle panel), and on the difference of room temperature fluorescence emission spectra (bottom panel) of wild type *Synechocystis* cells in the presence of 10 μM DCMU and 1 mM KCN. The curves on the top panel were measured as described in the legend of Fig. 1, NPQ was calculated as described in the legend of Fig. 5, while the differences in the room temperature fluorescence emission spectra were calculated from raw spectra as described in the legend of Fig. 4. Note that the induction curve in the top panel was arbitrarily shifted upwards by 0.3 for clarity
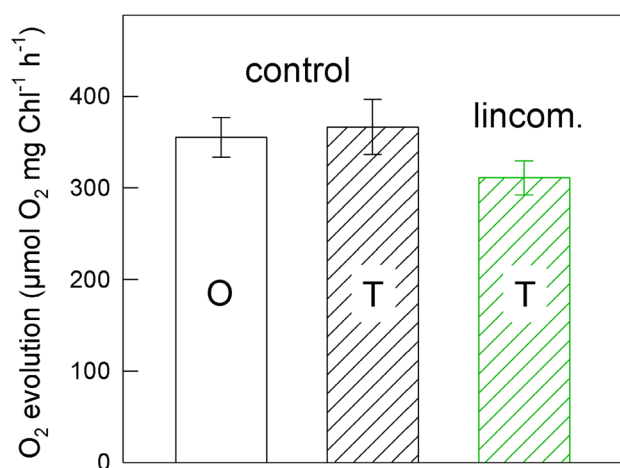
Fig. 9 Rate of oxygen evolution in wild type *Synechocystis* cells in the absence or in the presence of 1.5 mM lincomycin (lincom.). Cells were collected after 10 min of dark period [the O level (control); open column], as well as after 1800 s of the onset of the actinic light (the T level; striped columns; green for the sample with lincomycin). Average of three independent measurements with S.D. are shown

Discussion

As mentioned in the Introduction, the M–T fluorescence phase (P–T, when M is absent) is due to several processes; however, their relative contributions depend on the light intensity, the organism, the history, and the physiological, and stress conditions under which they are grown.

Following the early work of Papageorgiou et al. (2007), Kaňa et al. (2012) clearly established that state 2 to state 1 transition is responsible for the S–M fluorescence rise in cyanobacteria (also see Figs. 2, 3, this paper). We know that whenever *Synechocystis* cells are already in state 1, orange or blue light can change these cells to state 2 (see, e.g. Schreiber et al. 1995, Kirilovsky et al. 2006, 2014). Thus, it is reasonable to expect that state 1 to state 2 transition can indeed lead to fluorescence decrease, contributing to the M–T phase. At M, the cells are in state 1; thus, to go to state 2, a shift in the PQ/PQH_2 redox equilibrium to a more reduced state is required. However, in our experiments, re-reduction of the PQ-pool via PS II can be excluded since electron transfer from water to the PQ pool was inhibited by the addition of DCMU. Likewise, contribution of state transitions is excluded in principle in the $\Delta apcD$ mutant that is incapable of state-transition (Figs. 2, 3, 4).

Undoubtedly, another well characterized cyanobacterial photo-protective/regulatory mechanism, i.e., quenching by OCP, is known to be a significant contributor to the M–T phase upon illumination with intense blue, blue–green or white light (El Bissati et al. 2000; Wilson et al. 2006; Kirilovsky et al. 2014). However, intense orange light, which does not trigger OCP conversion into its active form

(Rakhimberdieva et al. 2004), also induces considerable M–T decrease in both wild type and in OCP-less *Synechocystis* (Figs. 1, 2 and 3); thus, besides OCP-quenching and, in some cases, state 1 to state 2 transition, other mechanisms must also contribute to the observed phenomenon of the M–T decline.

Intense illumination is known to cause significant decrease of Chl F; thus, photoinhibition is expected to contribute to the M–T phase under high light (also see Kirilovsky et al. 1990; Wilson et al. 2006; Stamatakis and Papageorgiou 2014). Nevertheless, 30 min illumination with 750 μmol photons m^{-2} s^{-1} of orange light did not cause any detectable impairment of the photosynthetic oxygen evolution in untreated *Synechocystis* cells (Fig. 9); this leads us to conclude that the contribution of photoinhibition to the M–T decline in our case is minor. However, in the presence of the protein synthesis inhibitor lincomycin, we observed, as compared to the untreated cells, a ~15% decrease in the rate of oxygen evolution, which is comparable to the ~11% increase in fluorescence quenching (from 38 to 42%) during the M–T transition (Figs. 4, 8). (For a linear relationship between fluorescence quenching and O_2 evolution, see Sarvikas et al. 2010.) This, thus, confirms that under high light, photoinhibition indeed contributes to the M–T fluorescence decline.

Stoitchkova et al. (2007) and Tamary et al. (2012) have shown a third-type of photoprotective/regulatory mechanism in cyanobacteria: local heat-transient-induced, photon-dose-dependent excitonic decoupling of PBS from PS II. Results of 77 K and room temperature fluorescence emission spectra (Tamary et al. 2012) suggest that this decoupling process has at least two, not yet elucidated, subsequent phases. During its first phase, the 678–682 nm shoulder/peak (depending on excitation light) in the room temperature fluorescence emission spectra disappears (Stoitchkova et al. 2007; Tamary et al. 2012), quite similar to our data shown in Fig. 4. This decrease is accompanied by a relative increase in the PBS emission at 77 K (Stoitchkova et al. 2007; Fig. 7). This initial phase is followed by a second phase with an increase of the PBS emission observed at both room temperature and at 77 K (Tamary et al. 2012), which is accompanied by an increase in PBS fluorescence in the central cytoplasmic region (Tamary et al. 2012; Steinbach and Kaňa 2016). Both room temperature fluorescence emission spectra (Fig. 4) and confocal microscopy data (not shown) indicate that its significance in our case is negligible. Nonetheless, the initial phase of the proposed photo-protective/regulatory mechanism, i.e. energetic (and physical) decoupling of the PBS from PS II, which is on the timescale of the M–T decreasing phase, makes its contribution possible. The smaller antenna-size at the T level, as suggested by TL measurements (Fig. 6 and "Thermoluminescence (TL)" section) supports this

proposed excitonic decoupling concept. Small effective antenna cross section, in general, is known to protect against photoinhibition in both green algae and cyanobacteria (Polle et al. 2002; Bernát et al. 2009, and Kwon et al. 2013); thus, a decrease of the effective antenna size by excitonic decoupling of the PBS from PS II seems to be a useful strategy when the cells are exposed to strong light. Importantly, although this decoupling can certainly contribute to the M–T phase of Chl F, yet its contribution must be relatively small (see Fig. 7) under the conditions of our experiment. Thus, by taking into account that significant M–T decline was observed when other known quenching processes (i.e. state 1 to state 2 transition, OCP-quenching, photoinhibition) could be neglected, we suggest that an additional, regulatory process may also contribute to the M–T decay in *Synechocystis*. Flavodiiron (Flv) proteins, suggested to be involved in dissipating excess light energy, and, hence, in NPQ in some cyanobacteria (for a review, see Allahverdiyeva et al. 2015), could potentially be responsible for these processes. Indeed, Flv2/Flv4 has been proven to compete with OCP-mediated NPQ (Bersanini et al. 2014); thus, Flv-mediated NPQ could potentially contribute to the M–T fluorescence decay in *Synechocystis* grown under ambient CO_2. Further experiments are needed to test this hypothesis. Furthermore, reaction center-dependent quenching could also be involved in the M–T phase. For instance, our TL data (Fig. 6) are also consistent with the hypothetical activation of a non-radiative pathway of charge recombination, which could harmlessly dissipate excess light energy. Such a flexible regulation is known in *Synechocystis*; however, it is via upregulation of the gene expression of certain D1 isoforms (Cser and Vass 2007). Similar photoprotective strategy has been suggested to be active in the red alga *Cyanidioschyzon merolae* (Krupnik et al. 2013). Finally, we cannot yet exclude that the recently described NPQ mechanism by Hlip (Staleva et al. 2015) is involved in the M–T fluorescence phase (for further details, see Acuña et al. 2016).

Regardless of its origin, this hypothetical mechanism must be much more prominent when other short-term responses are absent. This concept is in good agreement with the observed complex interplay of short-term regulatory responses in *Synechocystis* as well as in other cyanobacteria: (1) more pronounced S–M rise in OCP-less cyanobacterial strains indicating a more effective state 2 to state 1 transition (Kaňa et al. 2012; this work), (2) a more pronounced OCP-quenching in state transition-incapable strains (Jallet et al. 2012) and (3) a more pronounced M–T phase when these short-term responses are prevented (this work). Taken together, our data suggest that short-term processes play a photoprotective role and are in a complex and synergistic interrelationship with each other in order to maintain redox homeostasis of the cell.

References

Acuña AM, Kaňa R, Gwizdala M, Snellenburg JJ, van Alphen P, van Oort B, Kirilovsky D, van Grondelle R, van Stokkum IHM (2016) A method to decompose spectral changes in *Synechocystis* PCC 6803 during light-induced state transitions. Photosynth Res 130:237–249

Ajlani G, Vernotte C (1998) Construction and characterization of a phycobiliprotein-less mutant of *Synechocystis* sp. PCC 6803. Plant Mol Biol 37:577–580

Allahverdiyeva Y, Isojarvi J, Zhang P, Aro E-M (2015) Cyanobacterial oxygenic photosynthesis is protected by flavodiiron proteins. Life 5:716–743

Allakhverdiev SI, Nishiyama Y, Miyairi S, Yamamoto H, Inagaki N, Kanesaki Y, Murata N (2002) Salt stress inhibits the repair of photodamaged photosystem II by suppressing the transcription and translation of *psbA* genes of *Synechocystis*. Plant Physiol 130:1443–1453

Allakhverdiev SI, Nishiyama Y, Takahashi S, Miyairi S, Suzuki I, Murata N (2005) Systematic analysis of the relation of electron transport and ATP synthesis to the photodamage and repair of photosystem II in *Synechocystis*. Plant Physiol 137:263–273

Belgio E, Trskova E, Kotabova E, Ewe D, Prášil O, Kana R (2017) High light acclimation of *Chromera velia* points to photoprotective NPQ. Photosynth Res. doi:10.1007/s11120-017-0385-8

Bernát G, Waschewski N, Rögner M (2009) Towards efficient hydrogen production: the impact of antenna size and external factors on electron transport dynamics in *Synechocystis* PCC 6803. Photosynth Res 99:205–216

Bernát G, Appel J, Ogawa T, Rögner M (2011) Distinct roles of multiple NDH-1 complexes in the cyanobacterial electron transport network as revealed by kinetic analysis of P700$^+$ reduction in various *ndh*-deficient mutants of *Synechocystis* sp. Strain PCC6803. J Bacteriol 193:292–295

Bernát G, Schreiber U, Sendtko E, Stadnichuk IN, Rexroth S, Rögner M, Koenig F (2012) Unique properties vs. common themes: the atypical cyanobacterium *Gloeobacter violaceus* PCC 7421 is capable of state transitions and blue-light-induced fluorescence quenching. Plant Cell Physiol 53:528–542

Bersanini L, Battchikova N, Jokel M, Rehman A, Vass I, Allahverdiyeva Y, Aro E-M (2014) Flavodiiron protein Flv2/Flv4-related photoprotective mechanism dissipates excitation pressure of PSII in cooperation with phycobilisomes in cyanobacteria. Plant Phys 164:805–818

Bradbury M, Baker NR (1984) A quantitative determination of photochemical and non-photochemical quenching during the slow phase of the chlorophyll fluorescence induction curve of bean leaves. Biochim Biophys Acta 765:275–281

Briantais JM, Vernotte C, Krause GH, Weis E (1986) Chlorophyll *a* fluorescence of higher plants: chloroplasts and leaves. In: Govindjee, Amesz J, Fork DC (eds) Light emission by plants and bacteria. Academic Press, New York, pp 539–583

Brooks DM, Jansson S, Niyogi KK (2014) PsbS-dependent non-photochemical quenching. In: Demmig-Adams B, Garab G, Adams WW III, Govindjee (eds) Non-photochemical quenching and energy dissipation in plants, algae and cyanobacteria. Springer, Dordrecht, pp 297–314

Cser K, Vass I (2007) Radiative and non-radiative charge recombination pathways in Photosystem II studied by thermoluminescence and chlorophyll fluorescence in the cyanobacterium *Synechocystis* 6803. Biochim Biophys Acta 1767:233–243

Dall'Osto L, Caffari S, Bassi R (2005) A mechanism of nonphotochemical energy dissipation, independent from PsbS, revealed by a conformational change in the antenna protein CP26. Plant Cell 17:1217–1232

Dall'Osto L, Cazzaniga S, Wada M, Bassi R (2014) On the origin of a slowly reversible fluorescence decay component in the *Arabidopsis npq4* mutant. Trans R Soc B 369:20130221

Demmig-Adams B, Garab G, Adams WW III, Govindjee (2014) Non-photochemical quenching and energy dissipation in plants, algae and cyanobacteria. Springer, Dordrecht

DeVault D, Govindjee (1990) Photosynthetic glow peaks and their relationship with free-energy changes. Photosynth Res 24:175–181

El Bissati K, Delphin E, Murata N, Etienne AL, Kirilovsky D (2000) Photosystem II fluorescence quenching in the cyanobacterium *Synechocystis* PCC 6803: involvement of two different mechanisms. Biochim Biophys Acta 1457:229–242

Fratamico A, Tocquin P, Franck F (2016) The chlorophyll *a* fluorescence induction curve in the green microalga *Haematococcus pluvialis*: further insight into the nature of the P-S-M fluctuations and its relationship with the "low-wave" phenomenon at steady state. Photosynth Res 128:271–285

Garcia-Mendoza E, Ocampo-Alvarez H, Govindjee (2011) Photoprotection in the brown alga *Macrocystis pyrifera*: evolutionary implications. J Photochem Photobiol B 104:377–385

Govindjee, Amesz J, Fork DC (eds) (1986) Light emission by plants and bacteria. Academic Press, Orlando

Hamdani S, Qu M, Xin C-P, Li M, Chu C, Govindjee, Zhu X-G (2015) Variations between the photosynthetic properties of elite and landrace Chinese rice cultivars revealed by simultaneous measurements of 820 nm transmission signal and chlorophyll a fluorescence induction. J Plant Physiol 177:128–138

Holub O, Seufferheld MJ, Gohlke C, Govindjee, Heiss GJ, Clegg RM (2007) Fluorescence lifetime imaging microscopy of *Chlamydomonas reinhardtii*: non-photochemical quenching mutants and the effect of photosynthetic inhibitors on the slow chlorophyll fluorescence transient. J Microsc 226:90–120

Holzwarth AR, Jahns P (2014) Non-photochemical quenching mechanisms in intact organisms as derived from ultrafast-fluorescence kinetic studies. In: Demmig-Adams B, Garab G, Govindjee (eds) Non-photochemical quenching and energy dissipation in plants, algae and cyanobacteria. Springer, Dordrecht, pp 129–156

Horton P (2014) Developments in research on non-photochemical fluorescence quenching: emergence of key ideas, theories and experimental approaches. In: Demmig-Adams B, Garab G, Adams WW III, Govindjee (eds) Non-photochemical quenching and energy dissipation in plants, algae and cyanobacteria. Springer, Dordrecht, pp 73–95

Horton P, Hague A (1988) Studies on the induction of chlorophyll fluorescence in isolated barley protoplasts. IV. Resolution of non-photochemical quenching. Biochim Biophys Acta 932:107–115

Jallet D, Gwizdala M, Kirilovsky D (2012) ApcD, ApcF and ApcE are not required for the orange carotenoid protein related phycobilisome fluorescence quenching in the cyanobacterium *Synechocystis* PCC 6803. Biochim Biophys Acta 1817:1418–1427

Kaňa R, Govindjee (2016) Role of ions in the regulation of light-harvesting. Front Plant Sci 7:1849

Kaňa R, Přášil O, Komárek O, Papageorgiou GC, Govindjee (2009) Spectral characteristic of fluorescence induction in a model cyanobacterium, *Synechococcus* sp. (PCC 7942). Biochim Biophys Acta 1787:1170–1178

Kaňa R, Kotabová E, Komárek O, Šedivá B, Papageorgiou GC, Govindjee, Přášil O (2012) The slow S to M fluorescence rise in cyanobacteria is due to a state 2 to state 1 transition. Biochim Biophys Acta 1817:1237–1247

Kaňa R, Kotabová E, Lukeš M, Papáček Š, Matonoha C, Liu LN, Přášil O, Mullineaux CW (2014) Phycobilisome mobility and its role in the regulation of light harvesting in red algae. Plant Phys 165:1617–1631

Kirilovsky DL, Vernotte C, Etienne AL (1990) Protection from photoinhibition by low temperature in *Synechocystis* 6714 and in *Chlamydomonas reinhardtii*: detection of an intermediary state. BioChemistry 35:8100–8106

Kirilovsky D, Kaňa R, Přášil O (2014) Mechanisms modulating energy arriving at reaction centers in cyanobacteria. In: Demmig-Adams B, Garab G, Adams WW III, Govindjee (eds) Non-photochemical quenching and energy dissipation in plants, algae and cyanobacteria. Springer, Dordrecht, pp 471–501

Kodru S, Malavath T, Devadasu E, Nellaepalli S, Stirbet A, Subramanyam R, Govindjee (2015) The slow S to M rise of chlorophyll *a* fluorescence reflects transition from state 2 to state 1 in the green alga *Chlamydomonas reinhardtii*. Photosynth Res 125:219–231

Krupnik T, Kotabová E, van Bezouwen LS, Mazur R, Garstka M, Nixon PJ, Barber J, Kaňa R, Boekema EJ, Kargul J (2013) A reaction centre-dependent photoprotection mechanism in a highly robust photosystem II from an extremophilic red alga *Cyanidioschyzon merolae*. J Biol Chem 288:23529–23542

Küpper H, Andresen E, Wiegert S, Šimek M, Leitenmaier B, Šetlík I (2009) Reversible coupling of individual phycobiliprotein isoforms during state transitions in the cyanobacterium *Trichodesmium* analysed by single-cell fluorescence kinetic measurements. Biochim Biophys Acta 1787:155–167

Kwon JH, Bernát G, Wagner H, Rögner M, Rexroth S (2013) Reduced light-harvesting antenna: consequences on cyanobacterial metabolism and photosynthetic productivity. Algal Res 2:188–195

Laisk A, Oja V (2017) Kinetics of photosystem II electron transport: a mathematic analysis based on chlorophyll fluorescence induction. Photosynth Res. doi:10.1007/s11120-017-0439-y

Lemeille S, Rochaix JD (2010) State transition at the crossroad of thylakoid signaling pathways. Photosynth Res 106:33–46

Mao HB, Li GF, Ruan X, Wu QY, Gong YD, Zhang XF, Zhao NM (2002) The redox state of plastoquinone pool regulates state transitions via cytochrome b_6f complex in *Synechocystis* sp. PCC 6803. FEBS Lett 519:82–86

Minagawa J (2011) State transitions—the molecular remodeling of photosynthetic supercomplexes that controls energy flow in chloroplast. Biochim Biophys Acta 1807:897–905

Müller P, Li X-P, Niyogi KK (2001) Non-photochemical quenching; a response to excess light energy. Plant Physiol 125:1558–1566

Mullineaux CW, Allen JF (1986) The state 2 transition in the cyanobacterium *Synechococcus* 6301 can be driven by respiratory electron flow into the plastoquinone pool. FEBS Lett 205:155–160

Murchie EH, Harbinson J (2014) Non-photochemical fluorescence quenching across scales: From chloroplasts to plants to

communities. In: Demmig-Adams B, Garab G, Adams WW III, Govindjee (eds) Non-photochemical quenching and energy dissipation in plants, algae and cyanobacteria. Springer, Dordrecht, pp 553–582

Nedbal L, Trtílek M (1995) Diffuse-light dual-modulation fluorometer: monitoring of electron transfer reactions in *Synechococcus elongatus* exposed to intermittent light. In: Mathis P (ed) Photosynthesis: from light to biosphere, vol V. Kluwer, Dordrecht, pp 813–816

Nilkens M, Kress E, Lambrev PH, Miloslavina Y, Müller M, Holzwarth AR, Jahns P (2010) Identification of a slowly inducible zeaxanthin-dependent component of non-photochemical quenching of chlorophyll fluorescence generated under steady state conditions in *Arabidopsis*. Biochim Biophys Acta 1797:466–475

Ohad I, Raanan H, Keren N, Tchernov D, Kaplan A (2010) Light-induced changes within photosystem II protects *Microcoleus* sp. in biological desert sand crusts against excess light. PLoS ONE 5:e11000

Papageorgiou GC, Govindjee (1968) Light-induced changes in the fluorescence yield of chlorophyll *a in vivo* I. *Anacystis nidulans*. Biophys J 8:1299–1315

Papageorgiou GC, Govindjee (eds) (2004) Chlorophyll a fluorescence: a signature of photosynthesis. Advances in photosynthesis and respiration, vol 19. Kluwer Academic (now Springer), Dordrecht

Papageorgiou GC, Govindjee (2011) Photosystem II fluorescence: slow changes–scaling from the past. J Photochem Photobiol B 104:258–270

Papageorgiou GC, Tsimilli-Michael M, Stamatakis K (2007) The fast and slow kinetics of chlorophyll *a* fluorescence induction in plants, algae and cyanobacteria: a viewpoint. Photosynth Res 94:275–290

Polle JEW, Kanakagiri S, Jin E, Masuda T, Melis A (2002) Truncated chlorophyll antenna size of the photosystems—a practical method to improve microalgal productivity and hydrogen production in mass culture. Int J Hydrogen Energy 27:1257–1264

Prášil O, Bína D, Medová H, Řeháková K, Zapomělová E, Veselá J, Oren A (2009) Emission spectroscopy and kinetic fluorometry studies of phototrophic microbial communities along a salinity gradient in solar saltern evaporation ponds of Eilat, Israel. Aquat Microb Ecol 56:285–296

Puthiyaveetil S, Ibrahim IM, Allen JF (2012) Oxidation–reduction signalling components in regulatory pathways of state transitions and photosystem stoichiometry adjustment in chloroplasts. Plant Cell Environ 35:347–359

Rakhimberdieva MG, Stadnichuk IN, Elanskaya IV, Karapetyan NV (2004) Carotenoid-induced quenching of the phycobilisome fluorescence in photosystem II-deficient mutant of *Synechocystis* sp. FEBS Lett 574:85–88

Rappaport F, Lavergne J (2009) Thermoluminescence: theory. Photosynth Res 101:205–211

Samson G, Prášil O, Yaakoubd B (1999) Photochemical and thermal phases of chlorophyll *a* fluorescence. Photosynthetica 37:163–182

Sarvikas P, Tyystjarvi T, Tyystjarvi E (2010) Kinetics of prolonged photoinhibition revisited: Photoinhibited Photosystem II centres donot protect the active ones against loss of oxygen evolution. Photosynth Res 103:7–17

Schansker G, Tóth SZ, Holzwarth AR, Garab G (2014) Chloropyhll *a* fluorescence: beyond the limints of the Q_A model. Photosynth Res 120:454–463

Schreiber U. In: Van Kooten O (2002) Assessment of maximal fluorescence yield: donor-side dependent quenching and Q_B-quenching. In: Snel JFH (ed) Plant spectrophotometry: applications and basic research. Rozenberg Publishers, Amsterdam, pp 23–47

Schreiber U, Endo T, Mi H, Asada K (1995) Quenching analysis of chlorophyll fluorescence by the saturation pulse method: particular aspects relating to the study of eukaryotic algae and cyanobacteria. Plant Cell Phys 36:873–882

Serôdio J, Vieira S, Cruz S, Coelho H (2006) Rapid light-response curves of chlorophyll fluorescence in microalgae: relationship to steady-state light curves and non-photochemical quenching in benthic diatom-dominated assemblages. Photosynth Res 90:29–43

Staleva H, Komenda J, Shukla MK, Slouf V, Kana R, Polivka T, Sobotka R (2015) Mechanism of photoprotection in the cyanobacterial ancestor of plant antenna proteins. Nat Chem Biol 11:287–291

Stamatakis K, Papageorgiou GC (2014) ΔpH-dependent non-photochemical quenching (qE) of excited chlorophylls in the photosystem II core complex of the freshwater cyanobacterium *Synechococcus* sp PCC 7942. Plant Physiol Biochem 81:184–189

Stamatakis K, Tsimilli-Michael M, Papageorgiou GC (2007) Fluorescence induction in the phycobilisome-containing cyanobacterium *Synechococcus* sp PCC 7942: Analysis of the slow fluorescent transient. Biochim Biophys Acta 1767:766–772

Stanier RY, Kunisawa R, Mandel M, Cohen-Bazire G (1971) Purification and properties of unicellular blue-green algae (order *Chroococcales*). Bacteriol Rev 35:171–205

Steinbach G, Kaňa R (2016) Automated microscopy: Macro language controlling a confocal microscope and its external illumination: adaptation for photosynthetic organisms. Microsc Microanal 22:258–263

Stirbet A, Govindjee (2011) On the relation between the Kautsky effect (chlorophyll *a* fluorescence induction) and Photosystem II: Basics and applications of the OJIP fluorescence transient. J Photochem Photobiol B 104:236–257

Stirbet A, Govindjee (2012) Chlorophyll *a* fluorescence induction: a personal perspective of the thermal phase, the J-I-P rise. Photosyth Res 113:15–61

Stirbet A, Govindjee (2016) The slow phase of chlorophyll a fluorescence induction in silico: Origin of the S-M fluorescence rise. Photosynth Res 125:219–231

Stoitchkova K, Zsiros O, Jávorfi T, Páli T, Andreeva A, Gombos Z, Garab G (2007) Heat- and light-induced reorganizations in the phycobilisome antenna of *Synechocystis* sp. PCC 6803. Thermo-optic effect. Biochim Biophys Acta 1767:750–756

Strasser RJ, Srivastava A, Tsimilli-Michael M (2004) Analysis of the chlorophyll *a* fluorescence transient. In: Papageorgiou GC, Govindjee (eds) Chlorophyll *a* fluorescence: a signature of photosynthesis. Springer, Dordrecht, pp 321–362

Tamary E, Kiss V, Nevo R, Adam Z, Bernát G, Rexroth S, Rögner M, Reich Z (2012) Structural and functional alterations of cyanobacterial phycobilisomes induced by high-light stress. Biochim Biophys Acta 1817:319–327

Tsunoyama Y, Bernát G, Dyczmons NG, Schneider D, Rögner M (2009) Multiple Rieske proteins enable short- and long-term light adaptation of *Synechocystis* sp. PCC 6803. J Biol Chem 284:27875–27883

Tyystjärvi E (2013) Photoinhibition of Photosystem II. Int Rev Cell Mol Biol 300:243–303

Vass I, Govindjee (1996) Thermoluminescence of the photosynthetic apparatus. Photosynth Res 48:117–126

Vass I, Inoue Y (1992) Thermoluminescence in the study of photosystem II. In: Barber J (ed) The photosystems: structure, function and molecular biology. Elsevier, Amsterdam, pp 259–294

Vredenberg W, Prášil O (2013) On the polyphasic quenching kinetics of chlorophyll *a* fluorescence in algae after light pulses of variable length. Photosynth Res 117:321–337

Wilson A, Ajlani G, Verbavatz JM, Vass I, Kerfeld CA, Kirilovsky D (2006) A soluble carotenoid protein involved in phycobilisome-related energy dissipation in cyanobacteria. Plant Cell 18:992–1007

Wilson A, Punginelli C, Gall A, Bonetti C, Alexandre M, Routaboul JM, Kerfeld CA, van Grondelle R, Robert B, Kennis JTM, Kirilovsky D (2008) A photoactive carotenoid protein acting as light intensity sensor. Proc Natl Acad Sci USA 105:12075–12080